Self-assembly of a [2 × 2] hydrogen bonded grid

Piotr Lipkowski,[a] Anna Bielejewska,[a] Huub Kooijman,[b] Anthony L. Spek,[b]† Peter Timmerman*[a] and David N. Reinhoudt*[a]

[a] *Laboratory of Supramolecular Chemistry and Technology, MESA+ Research Institute, University of Twente, PO Box 217, NL-7500 AE Enschede, The Netherlands. E-mail: d.n.reinhoudt@ct.utwente.nl.*

[b] *Bijvoet Center for Biomolecular Research, Crystal and Structural Chemistry, Utrecht University, Padualaan 8, NL-3584 CH Utrecht, The Netherlands*

Received (in Liverpool, UK) 28th April 1999, Accepted 3rd June 1999

Formation of 24 cooperative hydrogen bonds drives the spontaneous assembly of a rigid bifunctional trimelamine and bis(barbituric acid) to give selectively the [2 × 2] hydrogen-bonded grid, in preference to the corresponding [1 × 1] or polymeric assemblies.

In 1992 Youinou and co-workers reported the formation of a $[Cu_4(dppn)_4](CF_3SO_3)_4$ complex in which the dppn [3,6-bis(2′-pyridyl)pyridazine] ligands are perpendicularly oriented pairwise around four Cu^+ centers thus forming a sandwich-type complex.[1] Very similar structures generally referred to as [$n \times n$] ‘metallosupramolecular grids’ have been reported by Lehn and co-workers.[2–4] Information storage both on the *covalent* and on the *supramolecular* level determines the overall size [$n \times n$] and shape (grid *vs.* helix) of the assembly.[5] We are currently investigating the self-assembly of [$n \times m$] hydrogen-bonded grids using the melamine–barbituric acid (M•BA) binding motif.[6] The formation of six cooperative hydrogen bonds between dimelamine **1** and 5,5-diethylbarbituric acid (DEB) ($K_{ass} = 7.6 \times 10^4$ M^{-1} in $CDCl_3$) restricts the rotations around the $C_{triazine}$–NH, the NH–CH_2, and the CH_2–C_{phenyl} bonds in **1**, giving the semi-rigid flat assembly **1**•DEB.[7] Here we describe the formation of [2 × 2] grid $\mathbf{2b}_2\bullet\mathbf{3}_2$, the simplest example of this type of hydrogen-bonded assemblies.[8] The grid has been fully characterized by 2D NMR spectroscopy, MALDI-TOF mass spectrometry, and vapor pressure osmometry (VPO).

The synthesis of trimelamine **2b** starts from cyanuric chloride *via* successive reactions with Bn_2NH (1.0 equiv.) and $BuNH_2$ (1.0 equiv.), followed by refluxing in neat *m*-xylylenediamine to give **4** in 92% yield (Scheme 1). Reaction of **4** with cyanuric chloride (0.5 equiv.) and subsequent aminolysis of the corresponding chloride **2a** with excess of NH_3 gives **2b** in 85% yield.[9] Bis(barbituric acid) derivative **3** was synthesized starting with the alkylation of diethyl 2-ethylmalonate with 1,3-diiodopropane in 35% yield,[10] followed by reaction with urea (NaOEt/EtOH) in 25% yield.[11]

Assembly of **2b** and **3** can in principle lead to three different hydrogen-bonded structures (see Scheme 1), *i.e.* the [1 × 1] assembly **2b•3**, the [2 × 2] (grid) assembly $\mathbf{2b}_2\bullet\mathbf{3}_2$, and the polymeric assembly $[\mathbf{2b}\bullet\mathbf{3}]_n$. Bis(barbituric acid) **3** was designed such that the formation of the [1 × 1] assembly, which would be preferred on entropic grounds,† is impossible. The short *n*-propyl spacer does not allow two barbituric acid moieties of one molecule of **3** to bind simultaneously to both binding sites of one molecule of **2b**. The X-ray crystal structure of free **3**‡ [see Fig. 1(*a*)] clearly confirms this picture and shows that the conformation adopted in the solid state is fully consistent with formation of the [2 × 2] grid $\mathbf{2b}_2\bullet\mathbf{3}_2$ [see Fig. 1(*b*)]. Furthermore, the high extent of preorganization in the monomeric units **2b** and **3** reduces the likelihood of hydrogen-bonded polymerization ($[\mathbf{2b}\bullet\mathbf{3}]_n$).

Addition of 1.0 equiv. of **2b** to a suspension of **3** in $CDCl_3$ results in rapid dissolution of both components. Conclusive evidence for the formation of assembly $\mathbf{2b}_2\bullet\mathbf{3}_2$ comes from VPO measurements which give an average MW of 2500, very close to the calculated MW of 2800.§ Furthermore, MALDI-TOF mass spectrometry after Ag^+ labeling[12] shows a small but distinct signal for the Ag^+ complex of $\mathbf{2b}_2\bullet\mathbf{3}_2$ (*m/z* 2924; calc. for $C_{152}H_{180}N_{44}O_{12}\bullet{}^{109}Ag^+ = 2924$) together with that for the (open) **2b•3** (not shown) (*m/z* 1517; calc. for $C_{76}H_{90}N_{22}O_6\bullet{}^{109}Ag^+ = 1517$). The presence of the latter is due to destruction of assembly $\mathbf{2b}_2\bullet\mathbf{3}_2$ upon addition of AgO_2CCF_3, most likely due to strong coordination of Ag^+ to the hydrogen-bonded triazine nitrogen.¶

The ^1H NMR spectrum of the 1:1 mixture of **2b** and **3** in $CDCl_3$ confirms the exclusive formation of the [2 × 2] grid $\mathbf{2b}_2\bullet\mathbf{3}_2$. The spectrum of $\mathbf{2b}_2\bullet\mathbf{3}_2$ at 60 °C [see Fig. 2(*a*)] shows a broad signal at δ14.0 (NH_{barb}), a singlet at δ 7.65 ppm (ArH) and two signals at δ 7.1 (NH_{xylyl} + ArH) and 6.76 (NH_{xylyl}). Both the NH_{butyl} and the NH_2 protons coincide with the aromatic proton signals for the four benzyl groups (δ 7.4–7.2). Furthermore, three singlets at δ4.84, 4.62 and 4.51 (CH_2Ar) and a doublet at δ3.33 [$NHCH_2(CH_2)_2CH_3$] are observed. At lower temperatures (< 30 °C), two signals are observed at δ 14.6 and 14.0, one broad and one sharp,‖ and a complex pattern of signals

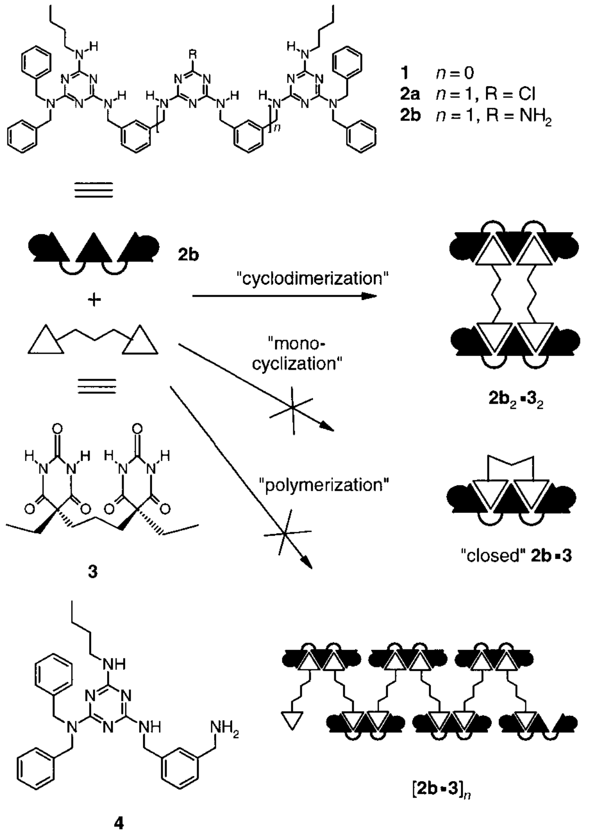

Scheme 1 Representation of the different types of hydrogen-bonded assemblies (*i.e.* [1 × 1], [2 × 2] and [$n \times n$]) that can be formed *via* hydrogen bond formation between trimelamine **2b** and bis(barbituric acid) **3**. Only the [2 × 2] assembly is experimentally observed.

---

† Address correspondence concerning crystallography to this author.

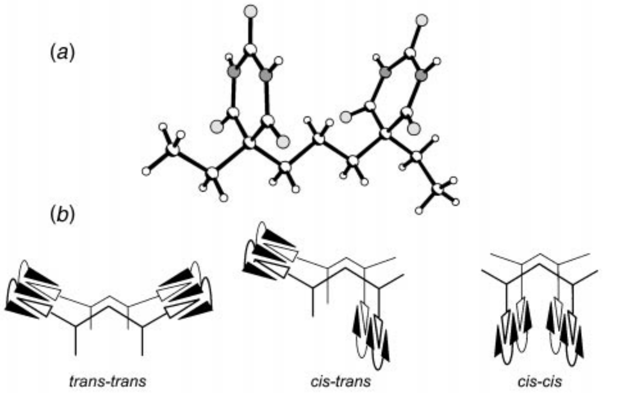

Fig. 1 (*a*) X-Ray crystal structure of **3**; white (small and large) atoms represent hydrogen and carbon atoms, grey (light and dark) atoms represent oxygen and nitrogen atoms. The barbiturate moiety [containing atom O(5)] is slightly distorted from planarity towards an envelope conformation (maximum deviation from the least-squares plane is 0.131(1) Å [for C(7)]). This distortion is most likely caused by the acceptance of intermolecular hydrogen bond formation [involving O(5) and O(6)]. (*b*) Three isomeric conformations of the [2 × 2] assembly $\mathbf{2b_2{\bullet}3_2}$.

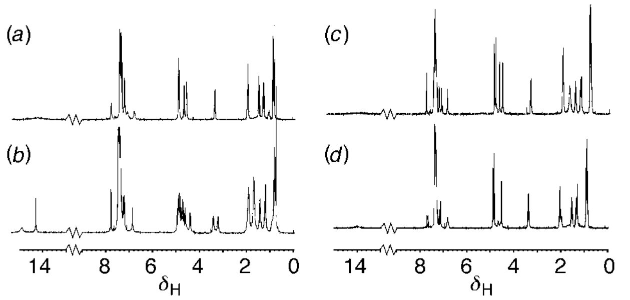

Fig. 2 ^{1}H NMR spectra (400 MHz) of (*a*) [2 × 2] assembly $\mathbf{2b_2{\bullet}3_2}$ at 60 °C; (*b*) [2 × 2] assembly $\mathbf{2b_2{\bullet}3_2}$ at −40 °C; (*c*) [1 × 2] assembly $\mathbf{2b}{\bullet}\mathrm{DEB}_2$ at −40 °C; (*d*) 1:1 mixture of [2 × 2] assembly $\mathbf{2b_2{\bullet}3_2}$ and [1 × 1] assembly $\mathbf{1}{\bullet}\mathrm{DEB}$ at 20 °C.

for the CH_2Ar protons and for the $NHCH_2(CH_2)_2CH_3$ protons is observed [see Fig. 2(*b*)]. The absence of any other signals in the δ 15–13 region clearly rules out the presence of alternative assemblies (*i.e.* [1 × 1] or polymeric) or the existence of more than one isomeric form [*trans-trans*, *cis-trans* and *cis-cis*, see Fig. 1(*b*)]. The less symmetrical *cis-trans* isomer can be ruled out based on symmetry arguments, but which of the two other isomers is the most stable one is at present unknown.

The decoalescence of the proton signals for the two heterotopic NH_{barb} protons around 30 °C clearly illustrates the much higher kinetic stability of grid $\mathbf{2b_2{\bullet}3_2}$ compared to assembly $\mathbf{2b}{\bullet}\mathrm{DEB}_2$, which shows an averaged (broad) signal around δ 14.0 for these two protons even at −50 °C [see Fig. 2(*c*)]. The reason is that exchange of these protons in $\mathbf{2b_2{\bullet}3_2}$ involves the simultaneous cleavage of 12 hydrogen bonds, while exchange in $\mathbf{2b}{\bullet}\mathrm{DEB}_2$ only requires six hydrogen bonds to be broken. Interestingly, the exchange between the two NH_{barb} protons in $\mathbf{2b_2{\bullet}3_2}$ is significantly faster in the presence of an equivalent amount of the two-component assembly $\mathbf{1}{\bullet}\mathrm{DEB}$ [averaged signal around δ 14.0 is observed, see Fig. 2(*d*)]. This is due to the fact that components **1** and DEB temporarily occupy the non-hydrogen bonded sites in $\mathbf{2b}{\bullet}\mathrm{DEB}_2$ during the exchange process, thus decreasing the activition barrier for this process.[13]

Finally we studied the thermodynamic stability of $\mathbf{2b_2{\bullet}3_2}$ as compared to that of $\mathbf{2b}{\bullet}\mathrm{DEB}_2$ and $\mathbf{1_2{\bullet}3}$. The melting point index for hydrogen-bonded assemblies $I_{T_\mathrm{m}} = \mathrm{HB}/(N - 1)$ predicts that an equimolar mixture of [1 × 2] assembly $\mathbf{2b}{\bullet}\mathrm{DEB}_2$ (I_{T_m} = 6) and [2 × 1] assembly $\mathbf{1_2{\bullet}3}$ (I_{T_m} = 6) is thermodynamically unstable, and would rearrange to give preferentially the [2 × 2] assembly $\mathbf{2b_2{\bullet}3_2}$ (I_{T_m} = 8) and [1 × 1] assembly $\mathbf{1}{\bullet}\mathrm{DEB}$ (I_{T_m} = 6).[14] Analysis of the ^{1}H NMR spectrum of a 1:1 mixture of $\mathbf{2b}{\bullet}\mathrm{DEB}_2$ and $\mathbf{1_2{\bullet}3}$ clearly shows that neither one of the two assemblies is present. Diagnostic is the absence of the characteristic resonances at δ 7.0 and 4.7. This experiment confirms the assumption that the thermodynamic stability of grid $\mathbf{2b_2{\bullet}3_2}$ is significantly higher than that of $\mathbf{2b}{\bullet}\mathrm{DEB}_2$ and $\mathbf{1_2{\bullet}3}$. Further studies on how structural parameters influence the stability of [2 × 2] grids are currently in progress.

This work was supported in part (A. L. S.) by the Netherlands Foundation of Chemical Research (SON) with financial aid from the Netherlands Organisation for Scientific Research (NWO).

Notes and references

† Based on the melting point index for hydrogen-bonded assemblies $I_{T_\mathrm{m}} = \mathrm{HB}/(N - 1)$ (where HB = number of H-bonds in the assembly and N = number of monomeric units in the assembly) (ref. 14), the stability of [1 × 1] assembly $\mathbf{2b{\bullet}3}$ is higher (I_{T_m} = 12) than [2 × 2] assembly $\mathbf{2b_2{\bullet}3_2}$ (I_{T_m} = 8) and the polymeric assembly $[\mathbf{2b{\bullet}3}]_n$ (I_{T_m} = 6).

‡ *Crystal data* for **3**: $C_{15}H_{20}N_4O_6$, $M_r = 352.35$, colourless, block-shaped crystal (0.2 × 0.2 × 0.3 mm), triclinic, space group $P1$ (no. 2) with $a = 6.5364(6)$, $b = 10.8100(12)$, $c = 11.7511(12)$ Å, $\alpha = 79.960(5)$, $\beta = 85.799(6)$, $\gamma = 88.868(6)°$, $V = 815.38(14)$ Å^3, $Z = 2$, $D_c = 1.435$ g cm^{-3}, $F(000)$ 372, μ(Mo-Kα) = 0.1 mm^{-1}, 23889 reflections measured, 3717 independent, $R_{int} = 0.0582$, ($1.6 < \theta < 27.4°$, T = 150 K, Mo-Kα radiation, graphite monochromator, λ = 0.71073 Å) on an Enraf-Nonius Kappa-CCD area detector on rotating anode. Data were collected for Lp effects but not for absorption. The structure was solved by automated direct methods (SHELXS96). Refinement on F^2 was carried out by full-matrix least-squares techniques (SHELXL-96) for 286 parameters. Hydrogen atoms were located on a difference Fourier map and their coordinates were included as parameters in the refinement. Refinement converged at a final w$R2$ value of 0.0898, $R1$ = 0.0317 [for 3522 reflections with $F_o > 4\sigma(F_o)$], S = 1.023. A final difference Fourier showed no residual density outside –0.24 and 0.32 e Å^{-3}. CCDC 182/1276. See http://www.rsc.org/suppdata/cc/1999/1311/ for crystallographic data in .cif format.

§ The experimentally determined average MW is slightly lower than the calculated MW, because assembly $\mathbf{2b_2{\bullet}3_2}$ is in equilibrium with the free components **2b** and **3** (concentration dependant on association constant of the complex). Moreover, the presence of a small excess of one of the components [~5% deviation from exact 1:1 stoichiometry (w/w)] will further decrease the average MW.

¶ Destruction of assembly $\mathbf{2b_2{\bullet}3_2}$ by Ag^+ ions was confirmed independantly by ^{1}H NMR spectroscopic measurements, which show the gradual disappearance (over several hours) of the proton signals after the addition of AgO_2CCF_3.

‖ The broadness of these signals is related to the proton exchange rate with residual water present. The NH_{barb} proton bound to the *outer* melamine unit (δ 14.6) is much broader than the NH_{barb} proton bound to the *inner* melamine unit (δ 14.0), because this proton is more exposed to the solvent (breakage of 3 *vs.* 6 hydrogen bonds).

1 M.-T. Youinou, N. Rahmouni, J. Fischer and J. A. Osborn, *Angew. Chem., Int. Ed. Engl.*, 1992, **31**, 733.

2 P. N. W. Baxter, J.-M. Lehn, J. Fischer and M.-T. Youinou, *Angew. Chem., Int. Ed. Engl.*, 1994, **33**, 2284.

3 P. N. W. Baxter, J.-M. Lehn, B. Kneisel and D. Fenske, *Chem. Commun.*, 1997, 2231.

4 G. S. Hanan, D. Volkmer, U. S. Schubert, J.-M. Lehn, G. Baum and D. Fenske, *Angew. Chem., Int. Ed. Engl.*, 1997, **36**, 1842.

5 J.-M. Lehn, *Supramolecular Chemistry, Concepts and Perspectives*, VCH, Weinheim, 1995.

6 S.-K. Chang and A. D. Hamilton, *J. Am. Chem. Soc.*, 1988, **110**, 1318; J.-M. Lehn, M. Mascal, A. DeCian and J. Fischer, *J. Chem. Soc., Chem. Commun.*, 1990, 479; J. P. Mathias, E. E. Simanek, J. A. Zerkowski, C. T. Seto and G. M. Whitesides, *J. Am. Chem. Soc.*, 1994, **116**, 4316.

7 C. M. Marjo, unpublished results.

8 J. Yang, E. Fan, S. J. Geib and A. D. Hamilton, *J. Am. Chem. Soc.*, 1993, **115**, 5314.

9 J. P. Mathias, E. E. Simanek and G. M. Whitesides, *J. Am. Chem. Soc.*, 1994, **116**, 4326.

10 A. C. Cope, H. L. Holmes and H. O. House, *Org. React.*, 1957, **9**, 107.

11 E. Fischer and A. Dilthey, *Ann.* 1904, **335**, 334.

12 K. A. Jolliffe, M. Crego Calama, R. Fokkens, N. M. M. Nibbering, P. Timmerman and D. N. Reinhoudt, *Angew. Chem., Int. Ed.*, 1998, **37**, 1294.

13 J. Rao, J. Lahiri, L. Isaacs, R. M. Weis and G. M. Whitesides, *Science*, 1998, **280**, 708.

14 M. Mammen, E. E. Simanek and G. M. Whitesides, *J. Am. Chem. Soc.*, 1996, **118**, 12614.

Communication 9/03446C